Engineering Homochiral MOFs by Spatially Separating 1D Chiral Metal-Peptide Ladders: Tuning the Pore Size for Enantioselective Adsorption

Kyriakos C. Stylianou,[†] Laura Gómez,[‡] Inhar Imaz,[†] Cristobal Verdugo-Escamilla,[¤] Xavi Ribas[‡] and Daniel Maspoch[†§*]

ChemSusChem
Communications

Abstract: The reaction of the chiral dipeptide glycyl-*L(S)*-glutamate with Co(II) ions produces chiral ladders that can be used as rigid 1D building units. Spatial separation of these building units with linkers of different lengths allows engineering of homochiral porous MOFs with enhanced pore sizes, pore volumes and surface areas. This strategy enables the synthesis of a family of isoreticular MOFs in which the pore size dictates the enantioselective adsorption of chiral molecules (in terms of their size and enantiomeric excess).

Metal-Organic Frameworks (MOFs) have witnessed a rapid expansion over the last two decades mainly because of their pore tunability, which allows optimizing the storage, separation and conversion of desired molecules.[1] Pore characteristics (size, shape, chirality and chemical environment) are essential for such functions, as they dictate which molecules can enter the pores as well as the affinity of the molecules that are adsorbed within the pores.[2] One of the most effective ways to control the pore size in MOFs is via rational connection of pre-designed, rigid building units (0D clusters, 1D chains or 2D layers) through organic linkers.[3] This approach, known as *reticular synthesis*, judiciously uses increasingly long linkers to expand pre-existing MOF structures by separating their characteristic building units.[4] It can thus provide a series of isoreticular MOFs with larger pores. For instance, pores as large as 98 Å have been obtained for a series of MOFs isostructural to MOF-74 (or CPO-27) constructed by connecting their characteristic 1D Mg(II) oxide unit through sequentially longer organic linkers: from dihydroxy-terephthalate up to eleven phenyl rings.[5] Although several isoreticular MOF families have been reported, this approach has rarely been used to tune the pore size of homochiral MOFs.[6] To the best of our knowledge, reticular synthesis has been employed to generate a family of homochiral MOFs in which layers built up from Ni(II) ions and *L*-aspartic acid are linked by pillar N-donor ligands such as 4,4'-bipyridine (bipy) and longer analogs of it.[6a] In this case, although the pore size was increased, the pores were not accessible, as the use of ligands longer than bipy resulted in their crystallization within the pores, blocking these pores for sorption applications.[6b] This approach has also been used by Dybtsev *et al.* to generate a second family of isoreticular homochiral MOFs, in which the design of enhanced pore sizes enabled enantioselective adsorption of bulkier molecules that could not be adsorbed by the isoreticular MOFs with smaller pores.[6c,6d]

Amongst the several chiral ligands available,[7] naturally occurring peptides is an attractive family of chiral ligands that can be used for the synthesis of homochiral MOFs. They can be prepared using unlimited combinations of amino acids and therefore, they possess rich structural versatility and abundant coordination sites for metal binding. Although there are many peptides available, truly porous and robust peptide-based MOFs are still scarce. In fact, most of these MOFs show dynamic or compact structures since peptides are flexible and tend to fold due to their aliphatic nature.[8] These structural characteristics prevent their use for the separation of chiral molecules which is of great importance, particularly in the pharmaceutical industry.[7,9]

Here, we report the use of a chiral peptide, glycyl-*L*(*S*)-glutamate (***L*-GG**) (Fig. 1a), to construct a chiral and rigid ladder-type building unit (**Co-*L*-GG**) that we subsequently used in reticular synthesis. Specifically, we separated the unit spatially from its original non-porous assembly to obtain a series of isoreticular homochiral porous MOFs by using the bipy linker and extended versions of it. The resulting MOFs are based on non-interpenetrated networks, are robust upon guest removal and up to 320 ºC, and are permanently porous to CO_2 (pore volumes: 0.118 cm^3/g to 0.256 cm^3/g). We further show that the pore size in this family of homochiral MOFs dictates not only the size of the molecules that can be enantioselectively adsorbed, but also the adsorption efficiency, in terms of enantiomeric excess (ee).

We produced the 1D **Co-*L*-GG** ladder-building unit by reacting $Co(OAc)_2 \cdot (H_2O)$ and ***L*-GG** in a mixture of H_2O and MeOH (1:1) for 2 h at 80 ºC (Fig. 1b,c). The infinite ladder units are constructed from the connection of octahedral Co(II) centers through ***L*-GG** linkers. Each ***L*-GG** coordinates to three Co(II) centers, whereas each Co(II) center is bound to four O atoms (three from the carboxylate groups, and one from the carbonyl group) and one N atom (from the terminal amino group) of three consecutive ***L*-GG** linkers, and to one H_2O molecule, which points towards the neighbouring 1D chains along the *c*-axis. In this configuration, the Co(II) ions are positioned at the vertices of the **Co-*L*-GG** ladders (Fig. 1c). These ladders are stacked along the *a*-axis, and are strongly connected through several H-bonds (distances: 1.9 Å to 2.7 Å) involving the carboxylate and amino groups of the ***L*-GG** linkers of the neighbouring ladders (Fig. 1d,e and S2). The ladders are also H-bonded along the *c*-axis, where the coordinated H_2O molecule is H-bonded (distance = 2.0 Å) to a carboxylate group of the ***L*-GG** linker of an adjacent ladder (Fig. S1). This arrangement yields a compact structure that lacks void volumes and is stable up to 400 ºC, as confirmed by thermogravimetric analysis (TGA; Fig. S4).

Our strategy for accessing the aforementioned non-porous homochiral structure entails replacing the coordinated terminal H_2O molecules of the **Co-*L*-GG** units with 4,4'-bipyridine (bipy)-type linkers. Considering that the **Co-*L*-GG** units and their stacking are not affected by this process, these linkers are ideal for interlinking and spatially separating the 1D **Co-*L*-GG** units (and by extension, the entire 2D supramolecular stacked **Co-*L*-GG** layer) by a distance defined by the length of the linker used (Fig. 1f). Here, two neighbouring units are connected through the vertices of the ladders. The resulting homochiral frameworks ensure incorporation of channels, the dimensions of which are defined by the shortest distance between two linkers bound to two neighbouring vertices, and by the length of the linker. Moreover, the compactness of the 2D stacked **Co-*L*-GG** units prevents interpenetration, as there is not enough space for a bipy-type linker to penetrate them.

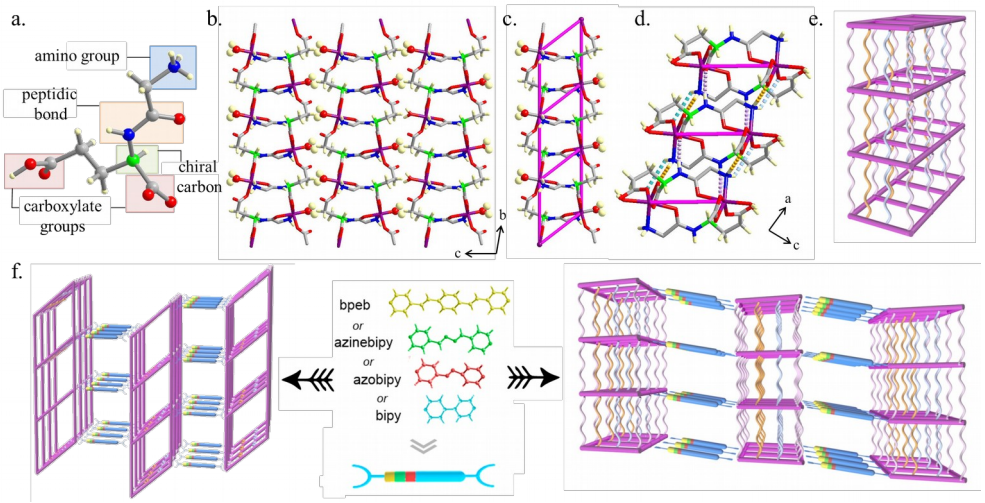

Figure 1. (a) Representation of the dipeptide ***L(S)*-GG**. (b) Illustration of the **Co-*L*-GG** ladders, highlighting the H_2O molecules (balls). (c) A single ladder-type **Co-*L*-GG** building unit (represented with pink sticks). (d) Representation of the H-bonding interactions occurred within three stacked **Co-*L*-GG** ladders along the *a*-axis. (e) Schematic representation of the repetitive supramolecular 2D stacked **Co-*L*-GG** units. H-bonds are shown as curved lines. (f) Schematic illustration of the strategy used to spatially separate the **Co-*L*-GG** building units using bipy-type linkers of different lengths. Left: view along the *a*-axis; right: view along the *b*-axis. Color code: O: red; N: blue; H: pale yellow; C: grey; Chiral C: green; and Co: purple.

Following the above strategy, we reproduced the same synthesis to obtain **Co-*L*-GG**, except that we introduced the bipy linker. Interestingly, single-crystal X-ray diffraction (XRD) performed on crystals collected from the mother liquor revealed formation of [Co-*L*-GG(bipy)$_{0.5}$]·(H_2O), **Co-*L*-GGbipy$_{_1}$**, in which the 2D stacked chiral **Co-*L*-GG** units (identical to those described in the **Co-*L*-GG** structure; Fig. 1d,e) were indeed interlinked by bipy linkers (Fig. 2a,b). Thus, the framework exhibited channels with dimensions of 3.5 x 5.2 Å (considering vdW radii), which were filled with guest H_2O molecules. Importantly, a fraction of **Co-*L*-GGbipy$_{_1}$** showed structural changes when it was exposed to the air. These changes involved a rotational disorder of the two pyridine rings of the bipy linker (Fig. S6,7). This disorder results in the loss of symmetry, leading to formation of **Co-*L*-GGbipy$_{_2}$**, which crystallizes in the triclinic *P*1 space group instead of the monoclinic *C*2 space group of **Co-*L*-GGbipy$_{_1}$**. Co-*L*-GGbipy$_{_2}$** showed the same framework topology, with slightly larger channels (3.6 x 5.7 Å, due to the torsion of the two pyridine rings of the bipy linker; Fig. 2c), a total accessible volume per unit cell of 15% (corresponding to 115 Å^3),[10] and a pore volume of 0.094 cm^3/g. Thus, when exposed to the air, a mixture of **Co-*L*-GGbipy$_{_1}$** and **Co-*L*-GGbipy$_{_2}$** coexisted. However, fully conversion to **Co-*L*-GGbipy$_{_2}$** was observed when this mixture was fully desolvated, as confirmed by powder X-ray diffraction (PXRD) (Fig. S9-11).

Seeking to expand the **Co-*L*-GGbipy** framework, we repeated the above synthesis, except that instead of bipy, we used longer analogs of it, including 4,4'-azobipyridine (azobipy), 4,4'-azinebipyridine (azinebipy) and 1,4-bis(4-pyridylethenyl)benzene (bpeb). Single-crystal XRD revealed that both **Co-*L*-GGazobipy** and **Co-*L*-GGazinebipy** are isoreticular frameworks with expanded pore apertures of dimensions of 3.3 x 6.2 Å and 3.2 x 6.9 Å (considering vdW radii), respectively (Fig. 2d,e), which corroborates the fact that azobipy and azinebipy are longer than bipy. The total accessible volume per unit cell of **Co-*L*-GGazobipy** is 25% (227 Å^3; pore volume: 0.126 cm^3/g), and of **Co-*L*-GGazinebipy**, 18% (157 Å^3; pore volume: 0.120 cm^3/g). Here, the inconsistency observed between the void volumes and the length of the two pillar ligands can be explained by the orientation of azobipy and azinebipy linkers in the structures. In **Co-*L*-GGazinebipy,** both pyridine rings of the azinebipy linkers point inside the channels and therefore, generate a smaller accessible pore volume than do the azobipy linkers in **Co-*L*-GGazobipy**.

We then explored even longer bpeb linkers, ultimately isolating intergrown flake-type crystals of **Co-*L*-GGbpeb** (Fig. 2f). Our efforts to grow larger crystals were not successful (Fig. S15), nor were our attempts to characterize the resulting crystals with synchrotron-radiation single-crystal XRD. Indexing the PXRD data of **Co-*L*-GGbpeb** with the software Topas 4.2 (Bruker AXS) yielded the following cell parameters: triclinic P1, a = 11.766(16) Å, b = 9.809(56) Å, c = 24.678(15) Å and α = 106.539(92)º, β = 100.03(10)º and γ = 81.94(19)º, which were refined through a Le Bail fitting procedure with excellent agreement indicators (Rwp = 3.36 %, Rp = 2.66 %, Rexp = 0.52 %), Fig. S16. These unit cell parameters are consistent with those derived from the single-crystal XRD of **Co-*L*-GGbipy$_{_2}$**, **Co-*L*-GGazobipy** and **Co-*L*-GGazinebipy**, confirming the formation of an isoreticular framework in which the *c*-axis is expanded to 24.679(15) Å. The only difference here is that the *a*-axis in **Co-*L*-GGbpeb** is twice as larger, which we reasoned was due to the asymmetry of two neighboring bpeb ligands running along this axis. Further evidence of the formation of the expanded isoreticular framework was also provided by elemental analysis, FT-IR and TGA. Elemental microanalysis suggested that the formula corresponds to the formation of a structure analogous to that of **Co-*L*-GGbipy$_{_2}$**, but which contains bpeb rather than bipy. The FT-IR spectrum of **Co-*L*-GGbpeb** revealed an almost identical fingerprint to that of the first three structures, with the characteristic C=O bands observed at comparable wavenumbers: **Co-*L*-GG**: 1698/1677 cm^{-1}; **Co-*L*-GGbipy$_{_2}$**: 1659/1650 cm^{-1}; **Co-*L*-GGazobipy**: 1662/1649 cm^{-1}; **Co-*L*-GGazinebipy**: 1661/1649 cm^{-1}; and **Co-*L*-GGbpeb**: 1660/1647 cm^{-1} (Fig. S17). Also, TGA revealed that **Co-*L*-GGbpeb** is stable up to 320 ºC; a fact consistent with the high thermal stability of **Co-*L*-GGbipy$_{_2}$**, **Co-*L*-GGazobipy** and **Co-*L*-GGazinebipy** (Fig. S18,20).

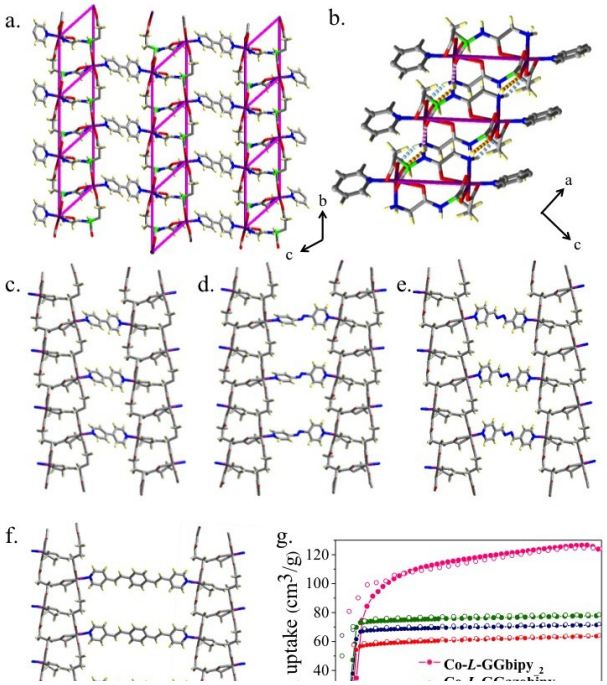

To evaluate the porosity of all the isoreticular frameworks, we performed N_2 and CO_2 gas sorption measurements at 77 K and 195 K, respectively. Prior to these measurements, all frameworks were activated at 40 ºC overnight under vacuum, and the activated samples were characterized by TGA and PXRD (Fig. S19,20). In all cases, TGA indicated a very small weight loss (<1%), which most likely arises from adventitious contamination by atmospheric water incurred during analysis, confirming that all MOFs pores were free of guest water molecules. Also, the simulated (derived from the single-crystal structures) and experimental (resulting from the activated samples) PXRD patterns were consistent, confirming their high structural integrity upon guest removal. N_2 isotherms on all four MOFs showed type II behaviour characteristic of non-porous materials. Contrariwise, the CO_2 adsorption isotherms of the four activated frameworks revealed that all of them are porous (Fig. 2g). This specific behaviour (porous to CO_2 and non-porous to N_2) is not scarce in MOFs. We reasoned that this selectivity could be due to the existence of structural defects, structural changes during gas adsorption, and/or the pore surface functionalization attracting and activating only quadrupolar molecules such as CO_2.[11]

Their CO_2 adsorption showed steep, stepwise uptake in the low-pressure region ($0<P<0.06$). In particular, the stepped CO_2 adsorption isotherms indicated that the frameworks are somewhat structurally flexible (*e.g.* phase transition and/or movements of the pillar ligands), consistently with structural observations of **Co-*L*-GGbipy$_{-1}$** and **Co-*L*-GGbipy$_{-2}$**.[8c,12] Above 0.06 bars, the CO_2 uptake of **Co-*L*-GGbipy$_{-2}$**, **Co-*L*-GGazobipy** and **Co-*L*-GGazinebipy** saturates, whereas upon increasing the pressure in **Co-*L*-GGbpeb**, it increases. The following Brunauer-Emmett-Teller (BET) surface areas were calculated from the CO_2 sorption data ($0.05 < p/p^0 < 0.3$): 261 m^2/g (**Co-*L*-GGbipy$_{-2}$**), 299 m^2/g (**Co-*L*-GGazobipy**), 315 m^2/g (**Co-*L*-GGazinebipy**) and 601 m^2/g (**Co-*L*-GGbpeb**). The observed pore volumes were: 0.118 cm^3/g (**Co-*L*-GGbipy$_{-2}$**), 0.146 cm^3/g (**Co-*L*-GGazobipy**), 0.166 cm^3/g (**Co-*L*-GGazinebipy**) and 0.256 cm^3/g (**Co-*L*-GGbpeb**). The pore volumes calculated from the CO_2 adsorption data are slightly greater than those calculated from the static structures, confirming that adsorption of CO_2 induces structural rearrangements (*e.g.* rotation of the pyridine rings of the pillar ligands).

Chiral MOFs with high surface areas and multiple active pore sites are highly desired for the resolution of racemic molecules of interest and enantioselective catalysis.[13] Herein, we have observed that the separation of the 2D stacked **Co-*L*-GG** units is reflected in the pore apertures, pore volumes and BET surface areas, all of which increase with increasing linker length. This tunability allows one to study how enantiomeric adsorption and separation are affected by pore aperture, by comparing MOFs that are structurally equivalent except for in terms of this parameter.[14] Our preliminary results in this area have shown that all the synthesized MOFs can enantioselectively adsorb a small molecule such as glycidol (volume: 110 $Å^3$), whereas only **Co-*L*-GGbpeb**, with its larger pore apertures, can enantioselectively adsorb a bulkier molecule such as hydrobenzoin (volume: 299 $Å^3$). Both molecules were enantioselective adsorbed in favour of the *S* form. These results have also shown that while the total amount of adsorbed glycidol tends to increase (from **Co-*L*-GGbipy$_{-2}$** to **Co-*L*-GGazobipy** and to **Co-*L*-GGazinebipy**) with increasing pore size and pore volume, the ee tends to decrease In the case of **Co-*L*-GGbpeb**, the ee is in comparable levels with that of **Co-*L*-GGazinebipy**

In the above experiments, we immersed each activated isoreticular MOF in a solution containing a racemic mixture of either glycidol or hydrobenzoin at room temperature. After 48 h, the crystals were filtered and washed with diethyl ether to remove any traces of surface bound molecules. All dried samples were immersed in anhydrous methanol and finally, heated at 40 ^oC for 4 h. This method allows for total extraction of adsorbed glycidol and hydrobenzoin without any harm to the MOFs, thereby enabling their re-use (*vide infra*). The amounts and ee's of glycidol and of hydrobenzoin in the extraction medium were measured using gas chromatography/mass spectrometry and high performance liquid chromatography, respectively. The detected amounts of adsorbed glycidol were 1.13 $mol_{glycidol}/mol_{MOF}$ in **Co-*L*-GGbipy$_{-2}$**, 1.31 $mol_{glycidol}/mol_{MOF}$ in **Co-*L*-GGazobipy**, 1.36 $mol_{glycidol}/mol_{MOF}$ in **Co-*L*-GGazinebipy** and 3.11 $mol_{glycidol}/mol_{MOF}$ in **Co-*L*-GGbpeb**. Inversely, the enantioselective adsorptions (*S*-glycidol over *R*-glycidol) were 54.1 ± 1.0% for **Co-*L*-GGbipy$_{-2}$**, 38.2 ± 2.0% for Co-*L*-GGazobipy, 34.0 ± 1.5 % for **Co-*L*-GGazinebipy** and 37.8 ± 1.0% for **Co-*L*-GGbpeb**. As previously mentioned, hydrobenzoin was adsorbed only by **Co-*L*-GGbpeb**, in the amount of 1.28 $mol_{hydrobenzoin}/mol_{MOF}$ and with an ee (*S*-hydrobenzoin over *R*-hydrobenzoin) of 24.1 ± 2.0 % (Table S3).

The aforementioned results confirmed that we could create isoreticular homochiral MOFs with controlled porosity and employ them to selectively tune enantioselective adsorption of chiral molecules. We would like to highlight two of our principal findings with this strategy. Firstly, by simply increasing the pore aperture in a given MOF, one can enantioselectively adsorb (and therefore, separate) chiral molecules of increasing size, as we observed with **Co-*L*-GGbpeb** and *S*-hydrobenzoin. Secondly, we observed an inverse correlation between the total amount of adsorbed glycidol and the enantioselective adsorption of the *S*-form: amongst the MOFs tested, **Co-*L*-GGbipy$_{-2}$** adsorbed the smallest amount of glycidol but exhibited the highest ee. We have posited that the smaller pore apertures of **Co-*L*-GGbipy$_{-2}$** might promote higher affinity (*i.e.* stronger interactions) between the glycidol and the chiral pore-wall surfaces.[15]

To provide evidence that the adsorbed *S*-enantioenriched glycidol or hydrobenzoin in these MOFs could be released without damaging them, we repeated twice the same glycidol adsorption process using a sample of **Co-*L*-GGbipy$_{-2}$** that we had pre-loaded once with glycidol and evacuated by immersion in methanol at 40 ºC. In these second and third processes, the total amounts of adsorbed glycidol were 1.09 and 1.04 $mol_{glycidol}/mol_{MOF}$, and the ee (*S*-glycidol over *R*-glycidol) was 54.4 ± 1.0 %

and 55.0 ± 1.5 %. The same process was repeated with the adsorption of hydrobenzoin in a sample of **Co-*L*-GGbpeb**, in which 3.01 and 3.08 $mol_{glycidol}/mol_{MOF}$ were adsorbed in the second and third cycle, with an ee (*S*-hydrobenzoin over *R*-hydrobenzoin) of 28.8 ± 4.0 % and 25.6 ± 0.5 % (Table S1). These results are comparable to those of the previous experiments, confirming that this isoreticular family of MOFs is sufficiently stable to be re-used for enantioselective adsorption, and that the adsorbed *S*-enantioenriched molecules can be fully released in methanol at 40 ºC, paving the way for their application in enantioseparation.

In conclusion, we have designed a family of isoreticular homochiral peptide-based MOFs through the linker extension strategy. These MOFs can be synthesized in high yields, and exhibit high thermal stabilities and permanent porosity, which can be tuned through judicious choice of the type and size of linker. The MOFs were further tested for the enantioselective adsorption of chiral molecules and proved that their separation is size dependent. This strategy has enabled us to better understand the formation and design peptide based MOFs for chiral separation applications.[7,9] Future studies will focus on extending the porosity of this isoreticular family of MOFs for the adsorption and separation of large drug-molecules in which the *R*- and *S*-enantiomers have different effects.

Notes and Supplementary Information

† ICN2 (ICN-CSIC), Institut Catala de Nanociencia i Nanotecnologia, Esfera UAB, 08193 Bellaterra, Spain

‡ Institut de Quimica Computacional i Catalisi (IQCC) and Departament de Quimica, Universitat de Girona, Campus Montilivi, E-17071 Girona, Catalonia, Spain

¤ Laboratorio de Estudios Cristalográficos, IACT, CSIC-Universidad de Granada, Av. de las Palmeras 4, E-18100 Armilla, Granada, Spain

§ Institució Catalana de Recerca i Estudis Avançats (ICREA), 08100 Barcelona, Spain; Email: daniel.maspoch@icn.cat

** Author to whom correspondence should be addressed.*

Electronic Supplementary Information is available on the WWW under http://dx.doi.org/10.1002/chem: synthetic details, PXRD, TGA, FT-IR and adsorption data are provided. The supplementary crystallographic data were deposited with the Cambridge Crystallographic Data Centre (CCDC) as entries 1033846 (**Co-*L*-GG**), 1033847 (**Co-*L*-GGbipy**$_1$), 1033848 (**Co-*L*-GGbipy**$_2$), 1033849 (**Co-*L*-GGazobipy**) and 1033850 (**Co-*L*-GGazinebipy**). These data can be obtained free of charge from the CCDC via www.ccdc.cam.ac.uk/data_ request/cif.

Acknowledgements

This work was supported by the MINECO-Spain under the project PN MAT2012-30994. I.I. thanks the MINECO for the RyC fellowship and K.C.S. is grateful to EU for the Marie Curie Fellowship (300390 NanoBioMOFs FP7-PEOPLE-2011-IEF). The authors thank Diamond Light Source for access to beamline I19, which contributed to the results presented herein (MT8477). X.R. thanks an ICREA.Acadèmia award. The project “Factoría de Cristalización, CONSOLIDER INGENIO-2010” provided PXRD facilities. ICN2 acknowledges support of the Spanish MINECO through the Severo Ochoa Centers of Excellence Program under Grant SEV-2013-0295.

Keywords: metal organic frameworks, peptides, chiral, porous, enantioselective separation, enantiomeric excess

[1] a) Allendorf, M. D.; Stavila, V. *Cryst. Eng. Comm.* **2015;** b) Furukawa, H.; Cordova, K. E.; O’Keeffe, M.; Yaghi, O. M. *Science* **2013**, 341; c) Makal, T. A.; Li, J.-R.; Lu, W.; Zhou, H.-C. *Chem. Soc. Rev.* **2012**, *41*, 7761; d) He, Y.; Zhou, W.; Qian, G.; Chen, B. *Chem. Soc. Rev.* **2014**, 43, 5657.

[2] a) Majumder, M.; Sheath, P.; Mardel, J. I.; Harvey, T. G.; Thornton, A. W.; Gonzago, A.; Kennedy, D. F.; Madsen, I.; Taylor, J. W.; Turner, D. R.; Hill, M. R. *Chem. Mat.* **2012**, 24**,** 4647; b) Queen, W. L.; Hudson, M. R.; Bloch, E. D.; Mason, J. A.; Gonzalez, M. I.; Lee, J. S.; Gygi, D.; Howe, J. D.; Lee, K.; Darwish, T. A.; James, M.; Peterson, V. K.; Teat, S. J.; Smit, B.; Neaton, J. B.; Long, J. R.; Brown, C. M. *Chem. Sci.* **2014**, 5, 4569; c) Kapelewski, M. T.; Geier, S. J.; Hudson, M. R.; Stuck, D.; Mason, J. A.; Nelson, J. N.; Xiao, D. J.; Hulvey, Z.; Gilmour, E.; FitzGerald, S. A.; Head-Gordon, M.; Brown, C. M.; Long, J. R. *J. Am. Chem. Soc.* **2014**, 136, 12119.

[3] a) Rosi, N. L.; Kim, J.; Eddaoudi, M.; Chen, B. L.; O’Keeffe, M.; Yaghi, O. M. *J. Am. Chem. Soc.* **2005**, 127, 1504; b) Liu, L.; Konstas, K.; Hill, M. R.; Telfer, S. G. *J. Am. Chem. Soc.* **2013**, 135, 17731.

[4] Yaghi, O. M.; O'Keeffe, M.; Ockwig, N. W.; Chae, H. K.; Eddaoudi, M.; Kim, J. *Nature* **2003**, 423, 705.

[5] Deng, H. X.; Grunder, S.; Cordova, K. E.; Valente, C.; Furukawa, H.; Hmadeh, M.; Gandara, F.; Whalley, A. C.; Liu, Z.; Asahina, S.; Kazumori, H.; O'Keeffe, M.; Terasaki, O.; Stoddart, J. F.; Yaghi, O. M. *Science* **2012**, 336, 1018.

[6] a) Vaidhyanathan, R.; Bradshaw, D.; Rebilly, J. N.; Barrio, J. P.; Gould, J. A.; Berry, N. G.; Rosseinsky, M. J. *Angew. Chem. Int. Ed.* **2006**, 45, 6495; b) Barrio, J. P.; Rebilly, J. N.; Carter, B.; Bradshaw, D.; Bacsa, J.; Ganin, A. Y.; Park, H.; Trewin, A.; Vaidhyanathan, R.; Cooper, A. I.; Warren, J. E.; Rosseinsky, M. J. *Chem. Eur. J.* **2008**, 14, 4521; c) Dybtsev, D. N.; Nuzhdin, A. L.; Chun, H.; Bryliakov, K. P.; Talsi, E. P.; Fedin, V. P.; Kim, K. *Angew. Chem. Int. Ed.* **2006**, 45, 916; d) Dybtsev, D. N.; Yutkin, M. P.; Samsonenko, D. G.; Fedin, V. P.; Nuzhdin, A. L.; Bezrukov, A. A.; Bryliakov, K. P.; Talsi, E. P.; Belosludov, R. V.; Mizuseki, H.; Kawazoe, Y.; Subbotin, O. S.; Belosludov, V. R. *Chem. Eur. J.* **2010**, 16, 10348.

[7] Nickerl, G.; Henschel, A.; Grünker, R.; Gedrich, K.; Kaskel, S. *Chem. Ing. Tech* **2011**, 83, 90.

[8] a) Imaz, I.; Rubio-Martinez, M.; An, J.; Sole-Font, I.; Rosi, N. L.; Maspoch, D. *Chem. Commun.* **2011**, 47, 7287; b) Marti-Gastaldo, C.; Warren, J. E.; Stylianou, K. C.; Flack, N. L. O.; Rosseinsky, M. J. *Angew. Chem. Int. Ed..* **2012**, 51, 11044; c) Rabone, J.; Yue, Y. F.; Chong, S. Y.; Stylianou, K. C.; Bacsa, J.; Bradshaw, D.; Darling, G. R.; Berry, N. G.; Khimyak, Y. Z.; Ganin, A. Y.; Wiper, P.; Claridge, J. B.; Rosseinsky, M. J. *Science* **2010**, 329, 1053.

[9] Li, X.; Chang, C.; Wang, X.; Bai, Y.; Liu, H. *Electrophoresis* **2014**, 35, 2733.

[10] a) Sheldrick, G. M. *SHELX97,* 1997, University of Göttingen, Göttingen, Germany; b) Spek, A. L. *J. Appl. Crystallogr*. **2003**, 36, 7.

[11] a) Masoomi, M. Y.; Stylianou, K. C.; Morsali, A.; Retailleau, P.; Maspoch, D. *Cryst. Growth Des.* **2014**, 14, 2092; b) Bhattacharya, B.; Haldar, R.; Dey, R.; Maji, T. K.; Ghoshal, D. *Dalton Trans.* **2014**, 43, 2272; c) McDonald, T. M.; Mason, J. A.; Kong, X.; Bloch, E. D.; Gygi, D.; Dani, A.; Crocella, V.; Giordanino, F.; Odoh, S. O.; Drisdell, W. S.; Vlaisavljevich, B.; Dzubak, A. L.; Poloni, R.; Schnell, S. K.; Planas, N.; Lee, K.; Pascal, T.; Wan, L. F.; Prendergast, D.; Neaton, J. B.; Smit, B.; Kortright, J. B.; Gagliardi, L.; Bordiga, S.; Reimer, J. A.; Long, J. R. *Nature* **2015**, *519*, 303.

[12] Zhang, Z.-X.; Ding, N.-N.; Zhang, W.-H.; Chen, J.-X.; Young, D. J.; Hor, T. S. A. *Angew. Chem. Int. Ed.* **2014**, 53, 4628.

[13] a) Peng, Y. W.; Gong, T. F.; Zhang, K.; Lin, X. C.; Liu, Y.; Jiang, J. W.; Cui, Y. *Nat. Commun.* **2014**, 5; b) Ma, L. Q.; Falkowski, J. M.; Abney, C.; Lin, W. B. *Nat. Chem.* **2010**, 2, 838; c) Yoon, M.; Srirambalaji, R.; Kim, K. *Chem. Rev.* **2012**, 112, 1196; d) Tanaka, K.; Kikumoto, Y.; Hota, N.; Takahashi, H. *New J. Chem.* **2014**, *38*, 880; e) Li, Z.-J.; Yao, J.; Tao, Q.; Jiang, L.; Lu, T.-B. *Inorg. Chem.* **2013**, *52*, 11694; f) Tanaka, K.; Muraoka, T.; Hirayama, D.; Ohnish, A. *Chem. Commun.* **2012**, *48*, 8577; g) Suh, K.; Yutkin, M. P.; Dybtsev, D. N.; Fedin, V. P.; Kim, K. *Chem. Commun.* **2012**, *48*, 513.

[14] a) Nuzhdin, A. L.; Dybtsev, D. N.; Bryliakov, K. P.; Talsi, E. P.; Fedin, V. P. *J. Am. Chem. Soc.* **2007**, 129, 12958; b) Das, M. C.; Guo, Q.; He, Y.; Kim, J.; Zhao, C.-G.; Hong, K.; Xiang, S.; Zhang, Z.; Thomas, K. M.; Krishna, R.; Chen, B. *J. Am. Chem. Soc.* **2012**, 134, 8703; c) Sawada, T.; Matsumoto, A.; Fujita, M. *Angew. Chem. Int. Ed.* **2014**, 53, 7228.

[15] Bradshaw, D.; Prior, T. J.; Cussen, E. J.; Claridge, J. B.; Rosseinsky, M. J. *J. Am. Chem. Soc.* **2004**, 126, 6106.

Entry for the Table of Contents

Layout 2:

COMMUNICATION

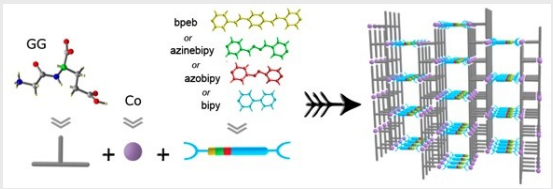

Engineering Homochiral MOFs by Spatially Separating 1D Chiral Metal-Peptide Ladders: Tuning the Pore Size for Enantioselective Adsorption

Kyriakos C. Stylianou, Laura Gómez, Inhar Imaz, Cristobal Verdugo-Escamilla, Xavi Ribas[‡] and Daniel Maspoch

Using the ligand extension strategy, we have engineered a family of porous homochiral peptide based Metal-Organic Frameworks. The control of their pore size dictates the enantioselective adsorption of chiral molecules in terms of their size and enantiomeric excess.